

# Investigations of Flowfield and Flame Structures in Recirculation Zone of Swirling Methane Jet Flames

T. S. Cheng<sup>1</sup>, Y.-C. Chao<sup>2</sup>, T.-C. Wu<sup>3</sup>, C.-Y. Wu<sup>2</sup>

<sup>1</sup>Department of Mechanical Engineering, Chung Hua University,  
Hsinchu, Taiwan, 300, ROC

<sup>2</sup>Institute of Aeronautics and Astronautics, National Cheng Kung University,  
Tainan, Taiwan, 701, ROC

<sup>3</sup>Department of Electronic Engineering, Kao Yuan University,  
Lujhu, Kaoshiung, Taiwan, 821, ROC

## 1 Introduction

The increasing stringent regulations have directed research efforts toward the reduction of pollutant emissions in various types of hydrocarbon combustion environments (e.g. aircraft jet engines, gas turbines for power generation, and utility boilers). Swirling flows are widely employed in industrial burners for increasing fuel-air mixing, intensifying and stabilizing combustion, shortening the flame length, and reducing pollutants. There is a large amount of studies on swirling flows [1, 2]; however, most attention is paid to the characteristics of the velocity fields and quite often intrusive measurement techniques using probes are applied. In order to gain a better understanding of the physical processes associated with mixing and combustion process and to provide quantitative data for CFD model validations, the detailed local fluid dynamic, thermodynamic, and chemical properties, such as velocity, mixture fraction, temperature, and species concentration, must be determined.

With advances in laser diagnostic techniques, the flowfield and flame properties in swirling flames can be obtained with high temporal and spatial resolutions. The flowfield can be measured by laser Doppler velocimetry (LDV) or particle imaging velocimetry (PIV), while the flame properties can be obtained with laser Rayleigh scattering, laser Raman scattering, or laser-induced fluorescence (LIF) or their combinations. Velocity, flame structure, and flame composition measurements, using LDV and Raman scattering techniques, in laboratory-scale swirling hydrogen flames [3], methane flames [4, 5], and natural gas flames [6] with different burner geometries have been reported. These measurements not only allow a better understanding of turbulence-chemistry interactions in the swirling flames, but also provide benchmark data set for combustion model validations.

In the present study, the flowfield and flame structures in recirculation zone of swirling methane/air flames ( $S = 1.0$ ,  $MR = 1.5$  and  $0.14$ ) with axial fuel injection are investigated. LDV is used to determine the fluid dynamic properties of the flowfields. UV Raman scattering and laser-induced predissociative fluorescence (LIPF) techniques are combined to simultaneously measure temperature, mixture fraction, major species ( $\text{CO}_2$ ,  $\text{O}_2$ ,  $\text{CO}$ ,  $\text{N}_2$ ,  $\text{CH}_4$ ,  $\text{H}_2\text{O}$ , and  $\text{H}_2$ ), and OH radical concentrations in the flames. Previously, velocity measurements in the flame with  $MR = 0.14$  were made at further downstream locations from the burner exit to study effects of fuel-air mixing on flame structures and pollutant emissions [4]. LDV measurements are re-performed at location near the burner exit where the measured data can be used as initial boundary conditions for numerical simulations.

## 2 Experimental setup

The experimental setup of the LDV system has been described elsewhere [4]. The UV line Raman/laser-induced predissociative fluorescence (LIPF) system is shown in Fig. 1. Details of the Raman system have been reported previously [7], and only a brief description is included in this paper. The Lambda-Physik LPX-250T narrowband KrF excimer laser produces light that is tunable from 247.9 to 248.9 nm with a bandwidth of  $\sim 0.003$  nm and a pulse energy of  $\sim 400$  mJ. The laser is tuned to 248.56 nm for major species and OH concentration measurements while keeps O<sub>2</sub> fluorescence signals minimum. Light scattered by the 2000 mm focusing lens is measured by a photomultiplier tube (PMT) to provide a relative measure of laser pulse energy. The laser beam is focused into either the flat-flame “Hencken” burner for calibration or the swirl burner for measurements. Fluorescence and Stokes Raman scattering signals are collected by two separate Cassegrain mirrors and focused into two spectrometers each coupled with an ICCD camera; the SPEX 500M spectrometer for measuring CO<sub>2</sub>, O<sub>2</sub>, CO, N<sub>2</sub>, and CH<sub>4</sub> and the Spectra Pro-275 spectrometer for detecting, H<sub>2</sub>O, H<sub>2</sub>, and OH. The Raman and fluorescence signals from the camera are digitized with a 14-bit A/D card connected to a personal computer for data processing. The camera image of the laser line is 3.31 mm in length, a value determined by the effective width of the CCD chip (7.8 mm) and the magnification of the collection optics (2.36). In post processing of data, the line image is divided into 8 segments, each with a spatial resolution of approximately 0.4 mm. The Raman/LIPF-OH imaging system is calibrated for all the 8 radial segments over the flat-flame burner at various stoichiometries. The well-calibrated Raman/LIPF-OH system is then used for analyzing the current swirling flames. The swirl burner is schematically shown in Fig. 2. The swirling component is generated by the swirler with six guide vanes at the angle of 45° or 55° which is placed coaxially with the central fuel tube, corresponding to the geometrical swirl number of 0.7 and 1.0, respectively. The diameter of the swirler is 30 mm. Methane can be supplied either from an axial injector with  $D = 5$  mm inner diameter or from an annular injector with four 2.5 mm holes inclined by 45° to investigate the effect of fuel injection. The swirl burner is mounted on a 2-D traversing table while the optical system remains fixed.

## 3 Results and discussion

Velocity and Raman scattering/LIPF measurements are performed in the radial direction at several downstream locations in swirling flames, which are operated with swirl number of  $S = 1.0$ , fuel-swirl air momentum flux ratio of  $MR = 1.5$  and  $0.14$ , and axial fuel injection. Here, we only report results (velocity, temperature, and mixture fraction) for three downstream locations ( $h = 2, 10, \text{ and } 20$  mm), due to space limitations. Figures 3 and 4 shows the radial profiles of turbulent kinetic energy and mean axial, radial, and tangential velocities at  $h = 2, 10, \text{ and } 20$  mm for  $MR = 1.5$  and  $0.14$ , respectively. For the fuel-jet dominated flame ( $MR = 1.5$ ), the centerline axial velocity is positive at all downstream locations indicating the penetration of fuel jet through the recirculation zone (Fig. 3). The first point of zero crossing of the axial velocity ( $r = 4$  mm) and the outer radial position of the peak velocity ( $r = 14$  mm) characterize the width of the recirculation zone. The location of the maximum radial velocity also indicates the lateral boundary of the recirculation zone. The maximum turbulent kinetic energy distributes near the edge of the recirculation zone indicating strong turbulent mixing at this location. For the strongly recirculating flame (Fig. 4), the centerline axial velocity is still positive at  $h = 10$  mm and becomes zero around  $h = 20$  mm, where is near the location of forward stagnation point.

The single-pulse species concentrations and temperatures are averaged over 200 laser shots. The mixture fraction is calculated from the measured species concentrations based on Bilger’s formulation [8] which preserves the stoichiometric value even in the presence of differential diffusion. Radial profiles of mean and rms temperatures at three downstream locations are shown in Fig. 5. The profiles show that for  $MR = 1.5$  the peak flame temperature appears at the mixing layer between the recirculation zone and the ambient air ( $r = 14$  mm) where the combustion products of H<sub>2</sub>O and CO<sub>2</sub> and the maximum turbulent kinetic energy occur. For the strongly recirculating flame ( $MR = 0.14$ ), a broader, uniform temperature distribution is observed. The temperature ranges from 1100 to 1300 K near the burner exit and decreases to 1000 K at  $h = 20$  mm. The uniformly low temperature ( $T < 1500$  K) could result in lower NO<sub>x</sub> emissions but may lead to higher CO emissions. Figure 6 shows the mixture fraction distributions for  $MR = 1.5$  and  $0.14$ . It can be seen that for the

fuel-jet dominated flame ( $MR = 1.5$ ) the centerline mixture fraction decays slowly, whereas for the strongly recirculating flame ( $MR = 0.14$ ), the centerline mixture fraction has decreased to fuel-lean condition at  $h = 20$  mm. It is noted that the maximum mixture fraction is not located at the jet centerline for  $MR = 0.14$  flame, due to the bending of fuel jet by the reversal flow.

## 4 Conclusions

Experimental measurements of velocity, temperature, and species concentration using LDV and UV Raman scattering/LIPF-OH techniques are made to investigate the flowfield and flame structure in the recirculation zone of swirling methane flames. Two distinct types of flames, fuel-jet dominated flame ( $MR = 1.5$ ) and strongly recirculating flame ( $MR = 0.14$ ), are investigated. Results indicate that the highly swirling flame produces rapid mixing, uniform temperature and mixture, and shortened flame length, which could lead to reduction of NO<sub>x</sub> emissions.

## Acknowledgement

This research was supported by the National Science Council of the Republic of China under the grant number NSC87-2212-E-216-007.

## References

- [1] Chigier NA et al. (1970). Jet flames in rotating flow fields. *Combust. Flame* 14: 171
- [2] Claypole TC, Syred N (1981). The effect of swirler burner aerodynamics on NO<sub>x</sub> formation. *Proc. Combust. Inst.* 18: 81
- [3] Tacke MM et al. (1996). Study of swirling recirculating hydrogen diffusion flame using UV Raman spectroscopy. *Proc. Combust. Inst.* 26: 169
- [4] Cheng TS et al. (1998). Effects of fuel-air mixing on flame structures and NO<sub>x</sub> emissions in swirling methane jet flames. *Proc. Combust. Inst.* 27: 1220
- [5] Weigand P et al. (2006). Investigations of swirl flames in a gas turbine model combustor I. Flow field, structure, temperature, and species distributions. *Combust. flame* 144: 205
- [6] Al-Abdeli Y, Masri A. (2003). Stability characteristics and flowfields of turbulent non-premixed swirling flames. *Combustion Theory and Modelling*, 7: 731
- [7] Cheng TS et al. (1998). Premixed methane-air flame spectra measurements using UV Raman scattering. *Combust. Sci. and Tech.* 135 : 65
- [8] Bilger RW (1988). The structure of turbulent nonpremixed flames. *Combust. Proc. Combust. Inst.* 22: 475

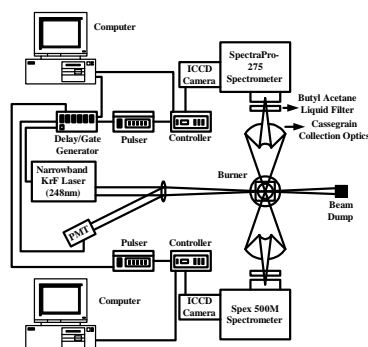


Fig. 1 Schematic diagram of the Raman/LIPF-OH system.

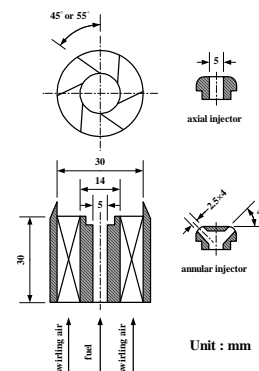


Fig. 2 Schematic diagram of the swirling burner.

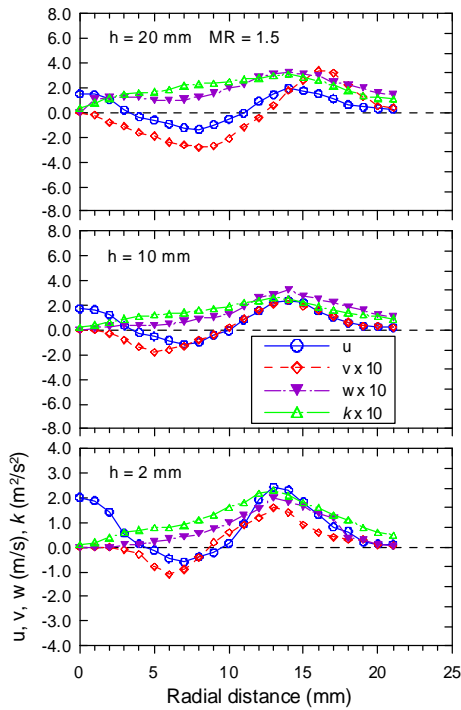


Fig. 3 Radial profiles of mean axial, radial, and tangential velocities and turbulent kinetic energy at three downstream tangential locations for MR = 1.5.

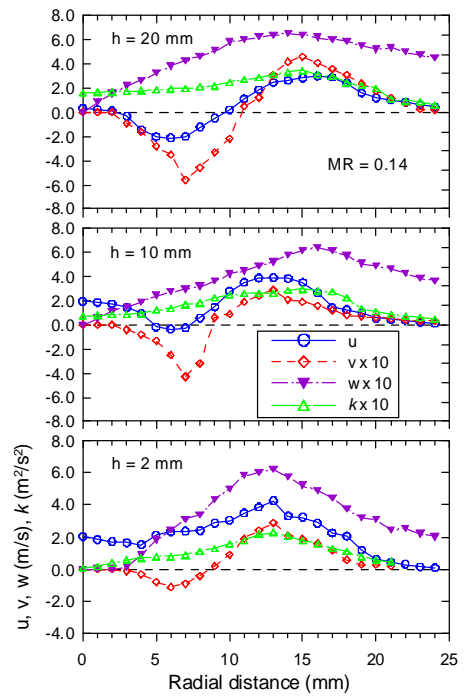


Fig. 4 Radial profiles of mean axial, radial, and tangential velocities and velocities and turbulent kinetic energy at three downstream locations for MR = 0.14.

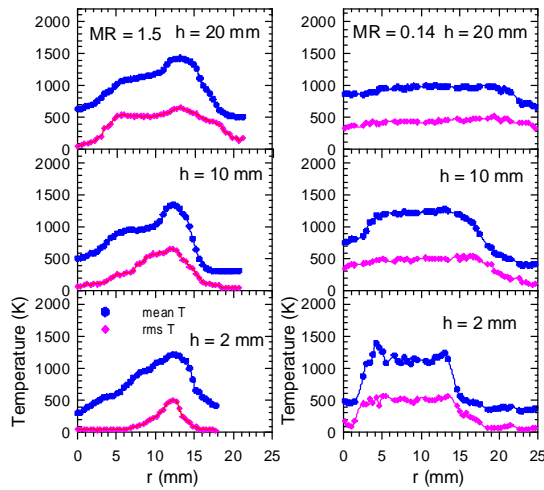


Fig. 5 Radial profiles of mean and rms temperature at three downstream tangential locations for MR = 1.5 and 0.14.

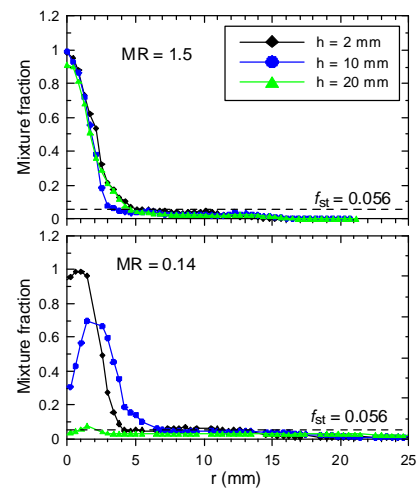


Fig. 6 Radial profiles of mean mixture fraction at three downstream tangential locations for MR = 1.5 and 0.14.